Expanding the Drosophila toolkit for dual control of gene expression

Jonathan Zirin[1,*], Barbara Jusiak[2,†], Raphael Lopes[1,†], Ben Ewen-Campen[1], Justin A. Bosch[1], Alexandria Risbeck[1], Corey Forman[1], Christians Villalta[1], Yanhui Hu[1], Norbert Perrimon[1,3,*]

1) Dept of Genetics, Harvard Medical School, Boston, MA
2) Dept of Physiology and Biophysics, University of California, Irvine, CA
3) Howard Hughes Medical Institute, Boston, MA

***** Corresponding authors
[†] These authors contributed equally to this work

Summary

The ability to independently control gene expression in two different tissues in the same animal is emerging as a major need, especially in the context of inter-organ communication studies. This type of study is made possible by technologies combining the GAL4/UAS and a second binary expression system such as the LexA-system or QF-system. Here, we describe a resource of reagents that facilitate combined use of the GAL4/UAS and a second binary system in various *Drosophila* tissues. Focusing on genes with well-characterizsed GAL4 expression patterns, we generated a set of more than 40 LexA-GAD and QF2 insertions by CRISPR knock-in and verified their tissue-specificity in larvae. We also built constructs that encode QF2 and LexA-GAD transcription factors in a single vector. Following successful integration of this construct into the fly genome, FLP/FRT recombination is used to isolate fly lines that express only QF2 or LexA-GAD. Finally, using new compatible shRNA vectors, we evaluated both LexA and QF systems for *in vivo* gene knockdown and are generating a library of such RNAi fly lines as a community resource. Together, these LexA and QF system vectors and fly lines will provide a new set of tools for researchers who need to activate or repress two different genes in an orthogonal manner in the same animal.

Introduction

Combinatorial binary systems

Most reagents available for loss of function (LOF) and gain of function (GOF) studies using RNAi or CRISPR rely on GAL4/UAS-mediated expression (Brand and Perrimon 1993; Dietzl et al. 2007; Perkins et al. 2015; Zirin et al. 2020; Port and Boutros 2022). However, some studies, such as the study of intercellular or inter-organ communication, require the simultaneous use of two independent binary transcriptional systems. For example, dual expression systems have been used to study how a *Drosophila* insulin-like peptide released from the wing primordium communicates with the brain to control organ growth (Colombani et al. 2015), analyze signaling from olfactory neurons to blood cells (Shim et al. 2013), independently manipulate ligand-producing and ligand receiving cells (Yagi et al. 2010), and visualize interactions between clonal cell populations in tissues (Bosch et al. 2015). Based on the need to simultaneously manipulate different sets of cells in a given tissue, the LexA/LexAop system (Lai and Lee 2006) and the QF/QUAS system (Potter et al. 2010; Potter and Luo 2011) have been developed. There have been no systematic studies comparing the two systems, with only anecdotal evidence to support one system over the other.

The numbers of available LexA and QF fly lines with tissue-specific expression domains are far lower than that represented by the thousands of GAL4 enhancer lines, which have been developed using various approaches over the past twenty-five years. The largest existing set of LexA system driver lines were produced by the Janelia FlyLight Project and Vienna Tiles Project (Jenett et al. 2012; Tirian and Dickson 2017). However, these lines were developed primarily for nervous system expression. Although they are often expressed in other tissues, they are not well suited for experiments targeting non-neuronal cell types. Furthermore, the FlyLight lines use a p65 transcriptional activation domain and therefore are not compatible with the Gal80 temperature sensitive Gal4 repression system. A second large collection of ~180 LexA-based enhancer trap fly stocks has been generated (the StanEx collection) (Kockel et al. 2016; Kockel et al. 2019; Kim et al. 2023). On average, each StanEx line expresses LexA activity in five distinct cell types, with only one line showing expression in just one tissue, unfortunately limiting usefulness of these reagents (Kockel et al. 2016). These findings are consistent with prior studies indicating that enhancers very rarely produce expression patterns that are limited to a single cell type in a complex organism (Jenett et al. 2012). Regarding the Q system, there are 101 total QF lines available from the Bloomington Drosophila Stock Center (BDSC). As the original QF can be toxic when expressed at high levels (Potter et al. 2010), second generation QF2 and QF2w, which are much less toxic and can be expressed broadly *in vivo* were generated (Riabinina et al. 2015). Among the 51 QF2 and QF2w lines available at BDSC, most are expressed in the brain, with relatively few of these drivers expressed specifically in other tissues. Thus, there remains an unmet need for more LexA and QF drivers with tissue-specific expression patterns. Furthermore, there are only ~260 LexA driver-compatible LexAop and ~130 QF driver-compatible QUAS stocks available at BDSC. The vast majority of these are to induce expression of fluorescent reporter genes, rather than molecular genetic reagents such as shRNAs for RNAi. This lack of fly stock reagents dramatically slows down studies that require two independent binary transcriptional systems, as custom fly stock reagents must be made by individual groups.

Rapid and efficient generation of driver lines by CRISPR-Cas9.

Several methods have been developed to generate new drivers with well-established tissue-specific patterns. However, these methods require either *de novo* generation of new driver lines, as for the integrase swappable *in vivo* targeting element (InSITE) system (Gohl et al. 2011), or PhiC31-induced insertion of a transcription factor cassette into an existing minos-mediated integration cassette (MiMIC) genomic insertion (Venken et al. 2011; Diao et al. 2015; Gnerer et al. 2015). CRISPR/Cas9 technology now makes it possible to knock-in a transcriptional activator into any locus. Some groups have also recently described tools to swap QF or LexA into the GAL4 coding region of existing GAL4 enhancer trap lines (Lin and Potter 2016; Chang et al. 2022; Karuparti et al. 2023). The conversion can be performed through genetic crosses; however, the frequency of conversion can vary greatly among different Gal4 lines, and many such swaps do not fully reproduce the original GAL4 expression patterns (Chen et al. 2019).

Despite these techniques, and the growing collection of LexA-GAD and QF2 lines, progress has been slow, and the choice of tissues depends on the specific interests of individual labs. Here, we describe the efforts of the Transgenic RNAi Project (TRiP) to facilitate combinatorial studies by building reagents that can be used alongside GAL4/UAS in a variety of tissues. Focusing on genes with well-characterized GAL4 expression patterns, we targeted 23 genes to produce 44 new highly tissue specific LexA-GAD and QF2 driver lines by CRISPR-mediated homology directed repair. We chose to use LexA with the Gal4 activation domain, rather than the p65 or VP16 activation domains to allow for temporal control by the temperature sensitive Gal4 repressor, Gal80 (Lai and Lee 2006; Pfeiffer et al. 2010). We chose to use QF2 variant over the original QF, to avoid the toxicity reported for the latter (Riabinina et al. 2015).

Like Gal80-based modulation of LexA-GAD, QF2 activity can also be regulated temporally by expressing QS, a QF repressor. QS repression of QF can be released by feeding flies quinic acid (Riabinina and Potter 2016). Each knock-in was rigorously genotyped, and the expression pattern verified by imaging. Thus, we can systematically compare LexA-GAD vs QF2 activators inserted at precisely the same position in the genome. In addition to the new fly stocks, we provide a new set of vectors and protocols to efficiently generate LexA-GAD and/or QF2 drivers. This includes constructs that encode QF2 and LexA-GAD transcription factors in a single vector, with each coding sequence flanked by FRT sites. Following successful integration into the fly genome, the vector generates a driver in which a target gene expresses both QF2 and LexA-GAD. If desired, one of the two coding regions can then be excised with Flp, resulting in flies that express only QF2 or LexA-GAD. Furthermore, we evaluated both QF2 and LexA-GAD systems for *in vivo* gene knockdown and are generating a compatible library of transgenic shRNA lines in our custom QUAS and LexAop vectors as a community resource. Together, these QF2/LexA-GAD and QUAS/LexAop vectors and fly lines will provide a new set of tools for researchers who need to activate or repress two different genes in an orthogonal manner in the same animal.

Results

Strategy for CRISPR knock-in of T2A-LexA-GAD and T2A-QF2.

We made each genetic driver line by inserting T2A-LexA-GAD or T2A-QF2 in the coding sequence of a target gene. We have previously reported the CRISPaint method to insert T2A-Gal4 into any gene using homology-independent repair (Bosch et al. 2020). Using this method, we showed robust gene-specific integration of donor plasmids in the fly germ line and successfully generated new driver lines. However, because of the high probability of indels at the insertion site, we opted to use traditional CRISPR homology-directed repair to insert the T2A-LexA-GAD and T2A-QF2 into the genome. We first modified the CRISPaint donor vectors to produce pHDR-T2A-LexA-GAD-Hsp70-3xP3-RFP and pHDR-T2A-QF2-Hsp70-3xP3-RFP, which contain the transcriptional activators followed by Hsp70 terminators. We opted to use the Hsp70 3'UTR, as opposed to SV40 3'UTR, because it is comparatively weaker and may avoid toxicity due to over-expression of LexA-GAD or QF2. We also constructed pHDR-T2A-QF2-T2A-LexA-GAD-3xP3-RFP, which contains both activators flanked by FRT sites followed by SV40 terminator **(Figure 1A)**. All the vectors contain a 3XP3-RFP transformation marker gene flanked by loxP sites. These vectors are compatible with two different cloning methods for making a CRISPR donor plasmid. In the long homology arm method (**Figure 1B)**, ~1000bp homology arms are amplified from genomic DNA and inserted into the donor plasmid by Gibson Assembly. A separate target-gene-specific guide RNA is cloned into a U6 promoter expression vector such as pCFD3 (Port et al. 2014). In the 'Drop-in' cloning method **(Figure 1C)** (Kanca et al. 2022), a company synthesizes and clones a plasmid that contains all of the necessary features for CRISPR HDR plus a cloning site to allow ligation of T2A-LexA-GAD, T2A-QF, or T2A-LexA-GAD-T2A-QF fragments in a single step to produce the donor plasmid.

For our targets, we selected a set of genes with tissue-specific expression patterns encompassing most of the major organs of the fly **(Table 1)**. When possible, we selected genes which had a previously characterized Gal4 insertion, and strong evidence of tissue specificity (e.g., from publicly available scRNAseq, *in situ*, and immunohistochemistry). Once the donors/guides were cloned, they were injected into Cas9-expressing fly embryos to induce CRISPR based HDR of the T2A-LexA-GAD or T2A-QF2 **(Figure 1D-E)**. We selected integration sites in the most 5' coding exon common to all or most isoforms, resulting in expression of the activators under control of the endogenous gene regulatory regions. The knock-in also produces a truncated endogenous protein and thus a predicted strong loss-of-function allele. To verify the

knock-ins, we PCR-amplified the genomic regions flanking the insertion sites and confirmed that the insertions were seamless and in-frame. Most of our knock-in stocks were made with the long homology arm method, but we transitioned to the Drop-in method as this technology became available. As **Table 1** shows, we were able to successfully generate knock-ins into nearly all the target genes using these methods.

Specificity of T2A-LexA-GAD and T2A-QF2 knock-in lines.

Next, we tested the specificity of the knock-in driver lines in the 3rd instar larva **(Figure 2)**. Each T2A-LexA-GAD and T2A-QF2 knock-in line was crossed to a LexAop-GFP and QUAS-GFP reporter, respectively. Note that most of the lines are highly tissue-specific and are comparable between the LexA-GAD and QF2 knock-ins. Insertions in the *daughterless* gene *(da)* are an exception, as the T2A-LexA-GAD **(Figure 2A)**, but not the T2A-QF2 **(Figure 2B)**, gives the expected ubiquitous expression pattern. Similarly, for insertions in the *nubbin* gene *(nub)* the T2A-LexA-GAD **(Figure 2LL)**, but not the T2A-QF2 **(Figure 2MM)**, gives the expected expression in the wing imaginal disc. In both cases, T2A-QF is expressed in the correct tissues, but incompletely. Even with these exceptions, the patterns are remarkably consistent between the T2A-LexA-GAD and T2A-QF2 knock-in lines overall.

Our donor plasmids contain the transgenesis marker 3XP3-RFP, which expresses red fluorescence in the larval gut and anal pad, and the adult eye (Berghammer et al. 1999). Like our previous knock-ins using the CRISPaint method (Bosch et al. 2020), we sometimes observed LexA-Gad or QF2 expression in the larval anal pad and gut, coincident with expression of RFP. **Figure 3** shows one such example in the *repo* gene, where T2A-QF2 is expressed in the expected glial cells, but also mis-expressed in RFP positive cells. Interestingly, this influence of the 3XP3-RFP is not observed in T2A-LexA-GAD *repo* knock-in animals **(Figure 2I)**. Conversely, in the *breathless (btl)* gene, we observe misexpression of LexA-GAD, but not QF2 in RFP positive cells **(Figure 2M-N)**. Importantly, when we removed the 3XP3-RFP cassette in the repo knock-in by cre-lox recombination, misexpression of QF2 in the gut and anal pad was completely eliminated, while the glial expression remained **(Figure 3B)**. We therefore have removed or are in the process of removing the 3XP3-RFP marker from all the knock-in stocks. Currently, we have successfully removed it from 32 of the 41 driver lines that used this marker **(Table 1)**.

T2A-QF2-T2A-LexA-GAD double driver lines

To make the T2A-LexA-GAD or T2A-QF2 knock-ins described above, each donor plasmid must be individually cloned and injected into embryos. We reasoned that by combining both drivers into a single construct we could halve the number of injections, one of the most labor-intensive and expensive parts of the process. For this combined expression of LexA-GAD and QF2 transcription factors, we built two types of vectors: 1) a CRISPR donor version, pHDR-T2A-QF2-T2A-LexA-GAD-3xP3-RFP, which is used to insert the cassette into an endogenous locus of interest **(Figure 4A)**, and 2) a phiC31-attB version, pMCS-T2A-QF2-T2A-LexA-GAD-WALIUM20, which is used to clone an enhancer fragment of interest and is then integrated into an attP site in the fly's genome **(Figure 4B)**. Note that the phiC31-attB compatible constructs use mini-white, not 3XP3-RFP as a marker gene. Using these vectors, we generated CRISPR knock-ins into the *elav* and *hedgehog (hh)* genes and enhancer lines for the *decapentaplegic (dpp)* and *Insulin-like peptide 2 (Ilp2)* **(Figure 4F)** genes. The *elav* knock-in **(Figure 4C)** expressed both T2A-QF2 and T2A-LexA-GAD in the expected pattern in the larval nervous system. However, we did see some weak non-specific expression of T2A-LexA-GAD in the somatic muscles. The *hh* knock-in **(Figure 4D),** expressed both T2A-QF2 and T2A-LexA-GAD in the expected pattern in the posterior of the imaginal discs. However, we observed that T2A-

QF2, but not T2A-LexA-GAD was restricted from the wing pouch, similar to the individual *nub* knock-ins **(Figure 4D and Figure 2LL-MM).** As expected, the *dpp* enhancer **(Figure 4E)** directed expression of both T2A-QF2 and T2A-LexA-GAD along the anterior/posterior margin of the wing imaginal disc. Again, however, T2A-QF was much reduced in the wing pouch. Finally, the *Ilp2* enhancer **(Figure 4F)** directed expression of both T2A-QF2 and T2A-LexA-GAD very specifically in the insulin-producing cells of the larval brain. Taken together, these results show that the double driver constructs can effectively drive expression of both activators simultaneously in the target tissue, with the caveat that T2A-QF2 does not express well in the wing pouch.

Next, we attempted to derive single T2A-QF2 and T2A-LexA-GAD lines from T2A-QF2-T2A-LexA-GAD double drivers. The strategy is outlined in **Figure 5A**. FRT3 and FRT are mutually incompatible target sites for the Flp recombinase: FRT3 can recombine with another FRT3, and FRT with FRT, but FRT3 cannot recombine with FRT. When recombined in *cis*, these mutually incompatible FRT target sites randomly excise one of two inserts (see Bosch et al. 2015). Hence, Flp expression will result in the formation of either T2A-$_{FRT3}$-LexA-GAD-$_{FRT}$ (caused by recombination between FRT3 sites) or T2A-$_{FRT3}$-QF2-$_{FRT}$ (if recombination occurs between FRT sites). Both recombination products will be stable even in the presence of Flp because they now lack a pair of compatible FRT sites. This enables us to obtain the individual driver lines (QF2 and LexA-GAD) by crossing the double drivers to flies that express Flp in the germline upon heat shock. We tested this with the *hh* and *dpp* lines and observed robust generation of both T2A-QF2 and T2A-LexA-GAD from *hs-Flp; T2A-QF2-T2A-LexA-GAD* parents **(Figure 5B)**. In the case of the *hh* line, 15 out of 36 heat-shocked parents gave rise to at least one T2A-LexA-GAD progeny, with a mean of 14% recombinant offspring per parent. 20 out of 36 gave rise to at least one T2A-QF2 progeny, with a mean of 9% recombinant offspring per parent. In the case of the *dpp* line, 31 out of 32 heat-shocked parents gave rise to at least one T2A-LexA-GAD progeny, with a mean of 30% recombinant offspring per parent. 17 out of 32 gave rise to at least one T2A-QF2 progeny, with a mean of 9% recombinant offspring per parent. We verified the recombinants by crossing to a stock containing both LexAop-mCherry and QUAS-GFP. **Figure 5C-E** shows the wing disc from the *hh* double driver **(Figure 5C)**, a recombinant which only expresses T2A-QF2 **(Figure 5D)** and a recombinant which only expresses LexA-GAD **(Figure 5E)**. Recombinants were also independently verified by PCR of the insertions **(Figure 5F-G),** where we observed the expected smaller band sizes in the derivative T2A-QF2 and T2A-LexA-GAD relative to the parental double driver.

TRiP LexAop and QUAS shRNA vectors produce effective gene knockdown.

The TRiP has previously generated a QUAS version of our standard shRNA expression vector, pQUAS-WALIUM20 (Perkins et al. 2015), containing the standard five copies of the QF binding site (Potter et al. 2010). We also generated pLexAop-WALIUM20, containing thirteen LexA DNA-binding sites, previously reported to give optimal expression with minimal leakiness (Pfeiffer et al. 2010) **(Figure 6A)**. We cloned shRNAs targeting *forked (f)* and *ebony (e)* genes into these vectors and assayed their phenotypes when crossed to ubiquitous LexA-GAD and QF2 drivers. The first driver tested was the T2A-LexA-GAD knock-in in the *da* gene **(Figure 2A)**, generated in this study. This produced 100% penetrant forked bristle and ebony cuticle phenotypes in the adult thorax when crossed to *f* **(Figure 6E)** and *e* **(Figure 6H)** shRNA lines, respectively. For this experiment, *white (w)* shRNA was used as a negative control. We did not test the T2A-QF2 knock-in in the *da* gene, as we have already shown that the expression pattern was not ubiquitous **(Figure 2G)**. Instead, to directly compare the two systems, we used previously described ubiquitous LexA-GAD and ubiquitous QF2 (Lai and Lee 2006) under the control of *αTub84B* regulatory sequences. Both Tub-LexA-GAD and Tub-QF2 drivers generated knockdown phenotypes in the thorax when crossed to *f* and *e* shRNA lines. However, the Tub-

LexA-GAD phenotypes were stronger than those of Tub-QF2 **(Figure 6C-D, F-G, I-J)**. For example, Tub-LexA-GAD produced a fully penetrant *f* bristle phenotype **(Figure 6F)** while some wild-type bristles remained on the thoraces of Tub-QF2 *f* knockdown **(Figure 6G)**. Neither Tub-LexA-GAD or Tub-QF2 was able to achieve the strength of phenotype generated by the T2A-LexA-GAD *da* knock-in line (compare the darkness of the cuticle caused by *e* knockdown in **Figure 6H-J**).

Discussion

There have been previous efforts to make LexA and QF tools, but the availability of LexA-GAD and QF2 tissue-specific fly stocks remains a major resource gap, preventing the average fly researcher from performing the type of multi-tissue manipulations that are essential to advance the study of organ and tissue communication. The collection of T2A-LexA-GAD and T2A-QF2 drivers described here is unique in that it is the first to focus on covering the major organ systems of the fly. Our protocol for generating these stocks is straightforward and can be easily adapted to produce driver lines for other fly tissues. These efforts will benefit from the emergence of scRNAseq datasets, which can be used to identify target genes with highly organ or tissue-specific gene expression patterns. For example, we identified the uncharacterized genes *CG9458* and *CG17560,* as highly oenocyte-specific based on the Fly Cell Atlas Single-cell transcriptome (Li et al. 2022), and the T2A-LexA-GAD and T2A-QF2 knock-ins in these genes were indeed restricted to this tissue. Our collection of T2A-LexA-GAD and T2A-QF2 and double driver vectors can be easily adapted to target any gene for CRISPR knock-in, with a high probability that the resulting line will accurately reflect the expression of the endogenous locus. The specificity achieved with this approach can also be seen in recent efforts to build collections of gene specific T2A-Split-Gal4 and T2A-Gal4 insertions (Kanca et al. 2019; Chen et al. 2023; Ewen-Campen et al. 2023). Our vectors are compatible with both the traditional large homology arm flanked cassettes and the more streamlined drop-in approach. In our hands, the drop-in cloning strategy is particularly effective, as the cloning success rate is 100%, requires little troubleshooting, has a very high knock-in rate, and only costs ~$100 to synthesize the construct (Kanca et al. 2019; Kanca et al. 2022).

Our results also present the opportunity to directly compare the LexA-GAD and QF2 systems. While we had no difficulty obtaining knock-ins for both types of activators, we did observe that for some target genes, the T2A-QF2 was only active in a subset of the expected gene expression pattern. In particular, we found that T2A-QF2 was difficult to express in the wing pouch. Additionally, we found that the driver expression in the gut-specific genes, *mex1* and *Myo31Df* differed between the LexA-GAD and QF2 transformants. In both cases the LexA-GAD was more broadly expressed along the length of the gut than the QF2. It may be that toxicity is an issue, and the weaker QF2w may be a better option for generating drivers in some organs (Riabinina and Potter 2016). Alternatively, differences in the LexA-GAD and QF2 sequences, and sequence length, could impact the function of nearby gene regulatory regions. Further, we expect that there will also be differences between the expression pattern of corresponding Gal4 and the LexA-GAD/QF lines, as the latter were made by knock-in, while the former are often enhancer traps. However, based on our larval mounts and dissections, the stocks generated in this paper are highly specific to the expression pattern of the targeted genes. Importantly, our knock-in constructs contain the 3XP3-RFP cassette for screening transformants. Perhaps due to interaction between the 3XP3 promoter and the regulatory regions of the target gene, we occasionally saw misexpression of the LexA-GAD/QF2 in the 3XP3 domain. We have therefore prioritized Cre-Lox removal of the 3XP3-RFP cassette from our knock-in stocks, and advise that users of the plasmids described here likewise remove the marker, following successful knock-in.

When we compared the knockdown efficiency of shRNAs targeting *forked* and *ebony* and, we found that the TRiP 13XLexAop vector was more effective than the 5XQUAS vector, although both were able to induce knockdown. Based on these results, the TRiP is currently generating a set of ~100 LexAop shRNA lines encompassing the genes targeted by the most commonly ordered UAS shRNA stocks at the BDSC. See **Supplementary File 1** for a list of all LexAop shRNA lines in production. There remains an unmet need for a single vector that would allow for UAS/LexAop/QUAS control of different shRNAs. However, recent innovations in multi module vectors and multiplexed drug-based genetics allow researchers to more efficiently generate UAS/QUAS/lexAop transgenic fly strains (Matinyan et al. 2021; Wendler et al. 2022). In summary, we have generated a set of stocks, vectors, and protocols that when combined with the wide array of GAL4 lines will greatly expand the ability of *Drosophila* researchers to modulate gene expression in multiple tissues simultaneously.

Materials and methods

Generation of pHDR-T2A-LexA/QF2-Hsp70-3xP3-RFP plasmids

To generate the pHDR-T2A-LexA/QF2-Hsp70-3xP3-RFP plasmids, we replaced the SV40-3'UTR present in the pCRISPaint-T2A-LexA/QF2 vector (Bosch et al. 2020) with the hsp70-3'UTR, using Gibson assembly (Gibson et al. 2009) (NEB E2611). The hsp70-3'UTR was amplified from a pCRISPaint-Gal4-Hsp70 plasmid using the following primers: F: GTCGACTAAAGCCAAATAG, R: AAACGAGTTTTTAAGCAAAC, appended at the 5' end with appropriate homologous overhangs for Gibson assembly. To remove the two endogenous SacI sites in the QF2 coding sequence, we used Gibson assembly featuring primers that introduce synonymous SNPs which mutate the SacI binding sites without disrupting the coding sequence (GAGCTC > GAACTC).

Cloning of T2A-LexA-GAD and T2A-QF2 donor constructs

For the long-homology arm cloning method, we amplified the homology arms (HAs) by selecting ~1000kb upstream and downstream of the guide cut site, making sure that the left HA is in frame with the T2A, and that the ends of the primers contain Gibson overhangs matching the pHDR-T2A-LexA/QF2-Hsp70-3xP3-RFP plasmids. Amplification was always from genomic DNA from the nos-Cas9 injection stock. We used Phusion (NEB), Taq (Takara) or Q5 (NEB). In cases where the PCR product was faint, we set up 8 PCR samples in parallel, combined them, concentrated them using phenol-chloroform extraction followed by ethanol precipitation, and ran the concentrated sample on a gel to obtain a bright band that was then gel-purified for use in Gibson Assembly. Once the HAs were amplified, we performed Gibson assembly with the pHDR-T2A-LexA/QF2-Hsp70-3xP3-RFP plasmids digested with AscI/SacI. Guide RNAs were cloned separately in pCFD3 (Port et al. 2014). We chose previously designed gRNAs from https://www.flyrnai.org/crispr3/web/. Our criteria were: efficiency >5, and no U6 termination site. Primer and guide sequences are in **Supplementary File 2**. We designed sense and antisense oligos for each gRNA, and then annealed them together to make a ds-oligo with overhangs for cloning: we combined 1.0 µl each 100 µM sense + antisense oligo, 1.0 µl 10x T4 ligase buffer, 0.5 µl T4 polynucleotide kinase (NEB), and 6.5 µl dH2O, and incubated at 37C 30 min followed by 5 min at 95C and slowly cooling down to room temperature (-5C/min). The ds-oligos were then ligated into BbsI-digested pCFD3 vector with T4 ligase (NEB). Following cloning, plasmids were verified by sequencing with primer (GCCGAGCACAATTGTCTAGAATGC).

For the Drop-in method, we followed a modified version of the protocol described elsewhere (Kanca et al. 2022). Briefly, homology donor intermediate vectors were ordered from Genewiz in the pUC57 Kan_gw_OK2 vector backbone, containing the gene-specific guide sequence, 200

bp short homology arms flanking the genomic cut site, and a BbsI and SacI cloning site. pHDR-T2A-LexA/QF2-Hsp70-3xP3-RFP plasmids were digested with AscI/SacI, producing a 2677 bp fragment for QF2 and the ~4.5kb fragment for LexA-GAD, each with overhangs compatible with the pUC57 Kan_gw_OK2 BbsI/SacI overhangs. The digested pUC57 Kan_gw_OK2 backbone, containing the homology arms and guides was then ligated with the digested T2A-LexA/QF2-Hsp70-3xP3-RFP with 2.5 µl 10× T4 DNA ligase buffer (NEB B0202S) and 0.5 µl T4 DNA ligase (NEB M0202S). Sequences of the synthesized Drop-in fragments are in **Supplementary File 3**.

Construction of T2A-QF2-T2A-LexA-GAD double driver constructs

For combined expression of LexA-GAD and QF2 transcription factors, we built two different vectors: 1) a CRISPR donor version, which we used to insert the LexA-GAD-QF2 cassette into an endogenous locus of interest, such that the expression of lexA-GAD and QF2 is driven by endogenous regulatory sequences, and 2) a ϕC31-attB version, which is used to clone an enhancer fragment of interest and integrated into an attP site in the fly genome.

To build the pHDR-T2A-QF2-T2A-LexA-GAD-3XP3-RFP construct, we used pCRISPaint-T2A-QF2 and pCRISPaint-T2A-LexA-GAD vectors (Bosch et al. 2020) to assemble the the vector as follows (See also **Supplementary File 4**):

1. A gBlock™ double-stranded DNA fragment covering the N-terminus of the QF2 ORF along with T2A, FRT3, and homology arms for Gibson assembly (BJusiak-QF2-N);
2. Part of the QF2 ORF amplified as a PCR product off the CRISPaint-T2A-QF2 vector using BJusiak-QF2-fwd+rev primer pair;
3. A gBlock™ encoding the C-terminus of QF2 and the FRTwt-T2A-FRT3 sequence between QF2 and LexA-GAD, along with homology arms for Gibson assembly (BJusiak-QF2-C);
4. Most of the LexA-GAD ORF, PCR-amplified off the CRISPaint-T2A-LexA-GAD template with the BJusiak-lexA1-fwd+rev primer pair;
5. BJusiak-FRToligo1-top+bottom, a pair of single-stranded oligos annealed to make a ds-oligo encoding the FRTwt site 3' of LexA-GAD;
6. CRISPaint vector digested with ApaI + KpnI restriction enzymes.

gBlocks™ and oligos were ordered from Integrated DNA Technologies (IDT) and restriction enzymes were from NEB. The sequences of all gBlocks™ and oligos used to build pHDR-QF2-LexA-GAD are in Supplementary materials and methods. Homology arms and guides for CRISPR were cloned as described above for the T2A-LexA-GAD and T2A-QF2 single donor constructs.

We digested CRISPaint-T2A-QF2 with ApaI at 25C in CutSmart buffer, followed by digestion with KpnI-HF at 37C. We ran the digest on an agarose gel and purified the 4.9 kb vector backbone. We then set up the Gibson Assembly:

Vector backbone (4,938 bp) 100 ng
lexGAD PCR product (2,875 bp) 117 ng 2:1 insert:vector molar ratio
QF2 PCR product (292 bp) 18 ng 3:1 insert:vector
BJusiak-QF2-N (713 bp) 44 ng 3:1 insert:vector
BJusiak-QF2-C (324 bp) 20 ng 3:1 insert:vector
FRT-ds-oligo (88 bp) 9.0 ng 5:1 insert:vector.

We added dH_2O to 10.0 µl final volume, added 10.0 µl Gibson Assembly Mix (NEB), and incubated at 50C for 1h. We transformed 5.0 µl of the Gibson Assembly reaction into Top10 chemically competent *E. coli* and plated on LB + Carbenicillin, then screened *E. coli* colonies by PCR with the BJusiak-Qlex-test1-fwd+rev primer pair (**Supplementary File 4**), expected to give a 0.7 kb product in presence of correctly assembled CRISPaint-QF2-lexGAD. Plasmid DNA was

prepared from positive colonies using the ZymoPure midiprep kit. Restriction digest fingerprinting of the plasmid midipreps produced expected band patterns, which were verified by sequencing.

To build the pMCS-T2A-QF2-T2A-LexA-GAD-WALIUM20 construct, we performed Gibson Assembly with the following fragments (See also **Supplementary File 4**):

1. MCS-WAL20-START gBlock™, including the MCS, hsp70 promoter, T2A-FRT3 coding sequence, and homology arms for Gibson assembly;
2. MCS-WAL20-STOP-v2 gBlock™, including the 3' end of LexA-GAD ORF, FRT coding sequence, and STOP codon;
3. QF2-T2A-LexA-GAD ORF PCR-amplified with FRT-QF2-fwd + FRT-lexA-GAD-rev primer pair – used Hot-Start Q5 polymerase with GC enhancer (NEB);
4. WALIUM20 vector digested with BamHI + EcoRI.

We transformed the Gibson Assembly reaction into Top10 chemically competent E. coli and plated them on LB + Carbenicillin. We screened colonies with PCR using the BJusiak-Qlex-test1-fwd+rev primer pair, same as for CRISPaint-QF2-lexGAD. Positive colonies were used for plasmid preps, which were sent for Sanger sequencing (Azenta) with the QF2-seq1-rev primer (TGTTAGTGAGATCAGCGAAC expected to read across the MCS-hsp70 region).
To make a variant pMCS-QF2-LexA-GAD-alt that lacks the Hsp70 promoter, we did Gibson assembly as above, except we replaced the MCS-WAL20-START with MCS-WAL20-START-new gBlock™, which lacks the Hsp70 sequence.

Cloning homology arms into pHDR-T2A-QF2-T2A-LexA-GAD-3XP3-RFP:

Homology arms were amplified by PCR as described above. See also **Supplementary File 5** for the PCR primers. We then digested pHDR-T2A-QF2-T2A-LexA-GAD-3XP3-RFP separately with AscI + SaCI to release the vector backbone and with NotI + SacI to purify the T2A-QF2-T2A-lexA-GAD-3XP3-RFP fragment. We gel-purified the backbone, T2A-QF2-T2A-lexA-GAD-3XP3-RFP fragment, and the homology arm PCR products, and we assembled all four fragments using Gibson Assembly. We used 50 ng vector backbone, 2-fold molar excess of T2A-QF2-T2A-lexA-GAD-3XP3-RFP, and 3-fold molar excess of each homology arm. We transformed the Gibson Assembly product into Top10 chemically competent E. coli, miniprepped (Qiagen) and verified by sequencing. Guides were cloned into pCFD3 as described above.

Cloning large enhancer fragments into pMCS-T2A-QF2-T2A-lexA-GAD-WALIUM20:

Ilp2-Gal4 has been described (Wu et al. 2005). The *dpp-blk* enhancer was described as a "4 kb BamHI fragment" (Masucci et al. 1990) that is 17 kb 3' of the *dpp* transcribed region (Blackman et al. 1987)(Blackman et al 1987). The primers used to PCR these fragments, using fly genomic DNA as template, are in **Supplementary File 6**. After PCR-amplifying the enhancer fragment with Q5 polymerase (+GC for *Ilp2*, no GC for *dpp*), we digested it and the destination vector with the corresponding enzymes (NotI + EcoRI for *dpp-blk*, PacI + EcoRI for *Ilp2*). We used pMCS-T2A-QF2-T2A-lexA0GAD-WALIUM20 for dpp-blk and pMCS-T2A-QF2-T2A-lexGAD-WALIUM20-alt (which lacks the hsp70 promoter) for *Ilp2*, since *dpp-blk* does not have a basal promoter, but the *Ilp2* enhancer does. We ligated the PCR fragments into the vectors using T4 ligase (NEB), transformed into *E. coli*, miniprepped (Qiagen) and verified by sequencing.

All vectors described here that are required to produce new driver lines will be made available at Addgene.

Cloning shRNAs

shRNAs (21 bp) were cloned into pQUAS-WALIUM20 and pLexAop-WALIUM20 vectors digested with digested with EcoRI + XbaI, as described previously (Ni et al. 2011). The oligos were as follows:

Gene	Oligo forward	Oligo reverse
white	ctagcagtCAGCGTCGTCCAGGTGCTGAAtagttatattcaagcataTTCAGCACCTGGACGACGCTGgcg	aattcgcCAGCGTCGTCCAGGTGCTGAAtagttatattcaagcataTTCAGCACCTGGACGACGCTGactg
ebony	ctagcagtTCCGGAGAGGTTCTTGGAGAAtagttatattcaagcataTTCTCCAAGAACCTCTCCGGAgcg	aattcgcTCCGGAGAGGTTCTTGGAGAAtagttatattcaagcataTTCTCCAAGAACCTCTCCGGAactg
forked	ctagcagtTCCGACCTAATTGCCGAGCTAtagttatattcaagcataTAGCTCGGCAATTAGGTCGGAgcg	aattcgcTCCGACCTAATTGCCGAGCTAtagttatattcaagcataTAGCTCGGCAATTAGGTCGGAactg

All transgenic lines were sequenced to confirm the identity of the shRNA.

Fly injections

All CRISPR constructs were injected at 250 ng/µl along with 100 ng/µl gene-specific gRNA(s) where appropriate. 300 embryos from *y w ; iso18; attP2, nos-Cas9* for genes on the X, second or fourth chromosomes and *y w ; attP40, nos-Cas9; iso5* for genes on the third chromosome per genotype were injected as described previously (Lee et al. 2018). Knock-in efficiencies were comparable to previous reports (Kanca et al. 2019; Kanca et al. 2022). Resulting G0 males and females were crossed individually to appropriate balancer flies for *3XP3-RFP* screening. Positive lines were balanced, and stocks were established. For phiC31-integration, each plasmid was injected at 50 ng/µl into *y v nos-phiC31-int; attP40* (for chromosome 2 insertions) or *y v nos-phiC31-int; attP2* (for chromosome 3 insertions). Injected male G0 flies were crossed with *y w; Gla/CyO or y w; Dr e/TM3, Sb* to identify transformants and remove the integrase from the X chromosome, and subsequently balanced.

PCR validation of knock-ins

PCR primers that flank the integration site were designed for each targeted gene. These primers were used in combination with primers that bind within the inserted cassette in both orientations. 500–800 nt amplicons were amplified from genomic DNA from individual insertion lines through single fly PCR using GoTaq green master mix (Promega M7122).

All transgenic fly stocks described here will be made available at the Bloomington Drosophila Stock Center.

Imaging

T2A-LexA-Gad, T2A-QF2, or double driver lines were crossed to *y w; Sp/CyO; LexAop-GFP (BDSC 52266), y w; QUAS-GFP/CyO (BDSC 52264), or y w; QUAS-GFP (BDSC 52264)/CyO-GFP; LexAop-RFP* (BDSC 52271*)/TM3*. Larvae were placed in PBS and sandwiched between a slide and coverslip, then live-imaged using a Zeiss (Carl Zeiss, Thornwood, NY) Stemi SVII fluorescence microscope. Wing imaginal discs from third instar larvae were dissected in PBS, fixed in 4% methanol free formaldehyde, and permeabilized in PBT, mounted on glass slides with vectashield (H-1000; Vector Laboratories) under a coverslip, and imaged on a Zeiss 780 confocal microscope.

Acknowledgements

We thank Stephanie Mohr for her support and advice on this project. This work was supported by 5P41GM132087 and 5R24OD030002. N.P. is an HHMI investigator. J.A.B. was supported by the Damon Runyon Foundation (DRG-2258-16) and a “Training Grant in Genetics” T32 Ruth Kirschstein-National Research Service Award institutional research training grant funded through the NIH/National Institute of General Medical Sciences (T32GM007748).

References

Berghammer AJ, Klingler M, Wimmer EA. 1999. A universal marker for transgenic insects. *Nature* **402**: 370-371. doi:10.1038/46463

Blackman RK, Grimaila R, Koehler MM, Gelbart WM. 1987. Mobilization of hobo elements residing within the decapentaplegic gene complex: suggestion of a new hybrid dysgenesis system in Drosophila melanogaster. *Cell* **49**: 497-505. doi:10.1016/0092-8674(87)90452-1

Bosch JA, Colbeth R, Zirin J, Perrimon N. 2020. Gene Knock-Ins in Drosophila Using Homology-Independent Insertion of Universal Donor Plasmids. *Genetics* **214**: 75-89. doi:10.1534/genetics.119.302819

Bosch JA, Tran NH, Hariharan IK. 2015. CoinFLP: a system for efficient mosaic screening and for visualizing clonal boundaries in Drosophila. *Development* **142**: 597-606. doi:10.1242/dev.114603

Brand AH, Perrimon N. 1993. Targeted gene expression as a means of altering cell fates and generating dominant phenotypes. *Development* **118**: 401-415. doi:10.1242/dev.118.2.401

Chang KR, Tsao DD, Bennett C, Wang E, Floyd JF, Tay ASY, Greenwald E, Kim ES, Griffin C, Morse E et al. 2022. Transgenic Drosophila lines for LexA-dependent gene and growth regulation. *G3 (Bethesda)* **12**. doi:10.1093/g3journal/jkac018

Chen YD, Chen YC, Rajesh R, Shoji N, Jacy M, Lacin H, Erclik T, Desplan C. 2023. Using single-cell RNA sequencing to generate predictive cell-type-specific split-GAL4 reagents throughout development. *Proc Natl Acad Sci U S A* **120**: e2307451120. doi:10.1073/pnas.2307451120

Chen YJ, Chang HH, Lin SH, Lin TY, Wu TH, Lin HJ, Liou NF, Yang CJ, Chen YT, Chang KH et al. 2019. Differential efficacy of genetically swapping GAL4. *J Neurogenet* **33**: 52-63. doi:10.1080/01677063.2018.1564289

Colombani J, Andersen DS, Boulan L, Boone E, Romero N, Virolle V, Texada M, Leopold P. 2015. Drosophila Lgr3 Couples Organ Growth with Maturation and Ensures Developmental Stability. *Curr Biol* **25**: 2723-2729. doi:10.1016/j.cub.2015.09.020

Diao F, Ironfield H, Luan H, Diao F, Shropshire WC, Ewer J, Marr E, Potter CJ, Landgraf M, White BH. 2015. Plug-and-play genetic access to drosophila cell types using exchangeable exon cassettes. *Cell Rep* **10**: 1410-1421. doi:10.1016/j.celrep.2015.01.059

Dietzl G, Chen D, Schnorrer F, Su KC, Barinova Y, Fellner M, Gasser B, Kinsey K, Oppel S, Scheiblauer S et al. 2007. A genome-wide transgenic RNAi library for conditional gene inactivation in Drosophila. *Nature* **448**: 151-156. doi:10.1038/nature05954

Ewen-Campen B, Luan H, Xu J, Singh R, Joshi N, Thakkar T, Berger B, White BH, Perrimon N. 2023. split-intein Gal4 provides intersectional genetic labeling that is repressible by Gal80. *Proc Natl Acad Sci U S A* **120**: e2304730120. doi:10.1073/pnas.2304730120

Gibson DG, Young L, Chuang RY, Venter JC, Hutchison CA, 3rd, Smith HO. 2009. Enzymatic assembly of DNA molecules up to several hundred kilobases. *Nat Methods* **6**: 343-345. doi:10.1038/nmeth.1318

Gnerer JP, Venken KJ, Dierick HA. 2015. Gene-specific cell labeling using MiMIC transposons. *Nucleic Acids Res* **43**: e56. doi:10.1093/nar/gkv113

Gohl DM, Silies MA, Gao XJ, Bhalerao S, Luongo FJ, Lin CC, Potter CJ, Clandinin TR. 2011. A versatile in vivo system for directed dissection of gene expression patterns. *Nat Methods* **8**: 231-237.

Jenett A, Rubin GM, Ngo TT, Shepherd D, Murphy C, Dionne H, Pfeiffer BD, Cavallaro A, Hall D, Jeter J et al. 2012. A GAL4-driver line resource for Drosophila neurobiology. *Cell Rep* **2**: 991-1001. doi:10.1016/j.celrep.2012.09.011

Kanca O, Zirin J, Garcia-Marques J, Knight SM, Yang-Zhou D, Amador G, Chung H, Zuo Z, Ma L, He Y et al. 2019. An efficient CRISPR-based strategy to insert small and large fragments of DNA using short homology arms. *Elife* **8**. doi:10.7554/eLife.51539

Kanca O, Zirin J, Hu Y, Tepe B, Dutta D, Lin WW, Ma L, Ge M, Zuo Z, Liu LP et al. 2022. An expanded toolkit for Drosophila gene tagging using synthesized homology donor constructs for CRISPR-mediated homologous recombination. *Elife* **11**. doi:10.7554/eLife.76077

Karuparti S, Yeung AT, Wang B, Guicardi PF, Han C. 2023. A toolkit for converting Gal4 into LexA and Flippase transgenes in Drosophila. *G3 (Bethesda)* **13**. doi:10.1093/g3journal/jkad003

Kim ES Rajan A Chang K Govindarajan S Gulick C English E Rodriguez B Bloomfield O Nakada S Beard C et al. 2023. Generation of LexA enhancer-trap lines in Drosophila by an international scholastic network. *G3 (Bethesda)*. doi:10.1093/g3journal/jkad124

Kockel L, Griffin C, Ahmed Y, Fidelak L, Rajan A, Gould EP, Haigney M, Ralston B, Tercek RJ, Galligani L et al. 2019. An Interscholastic Network To Generate LexA Enhancer Trap Lines in Drosophila. *G3 (Bethesda)* **9**: 2097-2106. doi:10.1534/g3.119.400105

Kockel L, Huq LM, Ayyar A, Herold E, MacAlpine E, Logan M, Savvides C, Kim GE, Chen J, Clark T et al. 2016. A Drosophila LexA Enhancer-Trap Resource for Developmental Biology and Neuroendocrine Research. *G3 (Bethesda)* **6**: 3017-3026. doi:10.1534/g3.116.031229

Lai SL, Lee T. 2006. Genetic mosaic with dual binary transcriptional systems in Drosophila. *Nat Neurosci* **9**: 703-709. doi:10.1038/nn1681

Lee PT, Zirin J, Kanca O, Lin WW, Schulze KL, Li-Kroeger D, Tao R, Devereaux C, Hu Y, Chung V et al. 2018. A gene-specific T2A-GAL4 library for Drosophila. *Elife* **7**. doi:10.7554/eLife.35574

Li H Janssens J De Waegeneer M Kolluru SS Davie K Gardeux V Saelens W David FPA Brbic M Spanier K et al. 2022. Fly Cell Atlas: A single-nucleus transcriptomic atlas of the adult fruit fly. *Science* **375**: eabk2432. doi:10.1126/science.abk2432

Lin CC, Potter CJ. 2016. Editing Transgenic DNA Components by Inducible Gene Replacement in Drosophila melanogaster. *Genetics* **203**: 1613-1628. doi:10.1534/genetics.116.191783

Masucci JD, Miltenberger RJ, Hoffmann FM. 1990. Pattern-specific expression of the Drosophila decapentaplegic gene in imaginal disks is regulated by 3' cis-regulatory elements. *Genes Dev* **4**: 2011-2023. doi:10.1101/gad.4.11.2011

Matinyan N, Karkhanis MS, Gonzalez Y, Jain A, Saltzman A, Malovannaya A, Sarrion-Perdigones A, Dierick HA, Venken KJT. 2021. Multiplexed drug-based selection and counterselection genetic manipulations in Drosophila. *Cell Rep* **36**: 109700. doi:10.1016/j.celrep.2021.109700

Ni JQ, Zhou R, Czech B, Liu LP, Holderbaum L, Yang-Zhou D, Shim HS, Tao R, Handler D, Karpowicz P et al. 2011. A genome-scale shRNA resource for transgenic RNAi in Drosophila. *Nat Methods* **8**: 405-407. doi:10.1038/nmeth.1592

Perkins LA, Holderbaum L, Tao R, Hu Y, Sopko R, McCall K, Yang-Zhou D, Flockhart I, Binari R, Shim HS et al. 2015. The Transgenic RNAi Project at Harvard Medical School: Resources and Validation. *Genetics* **201**: 843-852. doi:10.1534/genetics.115.180208

Pfeiffer BD, Ngo TT, Hibbard KL, Murphy C, Jenett A, Truman JW, Rubin GM. 2010. Refinement of tools for targeted gene expression in Drosophila. *Genetics* **186**: 735-755. doi:10.1534/genetics.110.119917

Port F, Boutros M. 2022. Tissue-Specific CRISPR-Cas9 Screening in Drosophila. *Methods Mol Biol* **2540**: 157-176. doi:10.1007/978-1-0716-2541-5_7

Port F, Chen HM, Lee T, Bullock SL. 2014. Optimized CRISPR/Cas tools for efficient germline and somatic genome engineering in Drosophila. *Proc Natl Acad Sci U S A* **111**: E2967-2976. doi:10.1073/pnas.1405500111

Potter CJ, Luo L. 2011. Using the Q system in Drosophila melanogaster. *Nat Protoc* **6**: 1105-1120. doi:10.1038/nprot.2011.347

Potter CJ, Tasic B, Russler EV, Liang L, Luo L. 2010. The Q system: a repressible binary system for transgene expression, lineage tracing, and mosaic analysis. *Cell* **141**: 536-548. doi:10.1016/j.cell.2010.02.025

Riabinina O, Luginbuhl D, Marr E, Liu S, Wu MN, Luo L, Potter CJ. 2015. Improved and expanded Q-system reagents for genetic manipulations. *Nat Methods* **12**: 219-222, 215 p following 222. doi:10.1038/nmeth.3250

Riabinina O, Potter CJ. 2016. The Q-System: A Versatile Expression System for Drosophila. *Methods Mol Biol* **1478**: 53-78. doi:10.1007/978-1-4939-6371-3_3

Shim J, Mukherjee T, Mondal BC, Liu T, Young GC, Wijewarnasuriya DP, Banerjee U. 2013. Olfactory control of blood progenitor maintenance. *Cell* **155**: 1141-1153. doi:10.1016/j.cell.2013.10.032

Tirian L, Dickson BJ. 2017. The VT GAL4, LexA, and split-GAL4 driver line collections for targeted expression in the Drosophila nervous system. *bioRxiv*: 198648. doi:10.1101/198648

Venken KJ, Schulze KL, Haelterman NA, Pan H, He Y, Evans-Holm M, Carlson JW, Levis RW, Spradling AC, Hoskins RA et al. 2011. MiMIC: a highly versatile transposon insertion resource for engineering Drosophila melanogaster genes. *Nat Methods* **8**: 737-743.

Wendler F, Park S, Hill C, Galasso A, Chang KR, Awan I, Sudarikova Y, Bustamante-Sequeiros M, Liu S, Sung EY et al. 2022. A LexAop > UAS > QUAS trimeric plasmid to generate inducible and interconvertible Drosophila overexpression transgenes. *Sci Rep* **12**: 3835. doi:10.1038/s41598-022-07852-7

Wu Q, Zhang Y, Xu J, Shen P. 2005. Regulation of hunger-driven behaviors by neural ribosomal S6 kinase in Drosophila. *Proc Natl Acad Sci U S A* **102**: 13289-13294. doi:10.1073/pnas.0501914102

Yagi R, Mayer F, Basler K. 2010. Refined LexA transactivators and their use in combination with the Drosophila Gal4 system. *Proc Natl Acad Sci U S A* **107**: 16166-16171. doi:10.1073/pnas.1005957107

Zirin J, Hu Y, Liu L, Yang-Zhou D, Colbeth R, Yan D, Ewen-Campen B, Tao R, Vogt E, VanNest S et al. 2020. Large-Scale Transgenic Drosophila Resource Collections for Loss- and Gain-of-Function Studies. *Genetics* **214**: 755-767. doi:10.1534/genetics.119.302964

Figure Legends

Figure 1: Strategy for CRISPR knock-in of T2A-LexA-GAD and T2A-QF2. (A) Donor vectors for knock-in. pHDR-T2A-LexA-GAD-Hsp70-3xP3-RFP and pHDR-T2A-QF2-Hsp70-3xP3-RFP contain T2A-LexA-GAD or QF2 transcriptional activators followed by HSP70 terminators. pHDR-T2A-QF2-T2A-LexA-GAD-3xP3-RFP contains both activators flanked by FRT sites followed by SV40 terminator. All the vectors contain a 3XP3-RFP transformation marker flanked by loxP sites. (B) Long homology arm cloning method. ~1000bp homology arms are amplified from genomic DNA and inserted into the AscI and SacI sites by Gibson Assembly. A separate target-gene-specific guideRNA is cloned into U6 promoter expression vector such as pCFD3. (C) Drop-in cloning method. Based on the gRNA-int200 method previously described (Kanca et al., 2022). A company synthesizes and clones a DNA fragment into the pUC57_Kan_gw_OK2 vector. The resulting plasmid contains the following elements: 1) two guide RNAs under the control of a U6 promoter, one (gRNA1) targeting the vector (pink arrows) to linearize the homology donor in vivo, and another ($gRNA^{geneX}$) targeting the gene of interest; 2) a tRNA sequence to allow liberation of the individual guides by the endogenous tRNA processing machinery; 3) 200 bp short homology arms; and 4) BbsI and SacI cloning sites. The AscI/SacI T2A-LexA-GAD, T2A-QF, or T2A-LexA-GAD-T2A-QF fragments can then be ligated in a single directional cloning step into the BbsI/SacI sites to produce the donor plasmid. (D) T2A-LexA-GAD and (E) T2A-QF2 knock-in strategy. CRISPR based HDR causes integration of the T2A-LexA-GAD or T2A-QF2 in the most 5' coding exon common to all or most isoforms, resulting in expression of the activators under control of the endogenous gene regulatory region. The knock-in also produces a truncated endogenous protein and thus a strong loss-of-function allele.

Figure 2: Tissue specificity of T2A-LexA-GAD and T2A-QF2 knock-ins.
(A-KK) T2A-LexA-GAD knock-in lines crossed to a LexAop-GFP reporter and T2A-QF2 knock-in lines crossed to a QUAS-GFP reporter. Panels show 3rd instar larva. GFP shows the driver line expression pattern. RFP shows the 3XP3 transformation marker, which labels the posterior gut and anal pads of the larva. Gene names and tissues are on the left. We failed to obtain LexA-GAD knock-ins for *Mef2* (E) and *He* (DD). (LL-MM) 3rd instar imaginal disc from the insertions in the *nubbin (nub)* gene. Note that most of the lines are highly tissue-specific and are comparable between the LexA-GAD and QF2 knock-ins. Insertions in the *daughterless* gene *(da) and nub* are an exception, as the T2A-LexA-GAD, but not the T2A-QF2, gives the expected expression pattern. Insertions in the gut-specific genes *mex1* (X-Y) and *Myo31Df* (Z-AA) also differed between the LexA-GAD and QF2 drivers.

Figure 3: 3XP3-RFP can cause misexpression of T2A-LexA-GAD or T2A-QF2. (A) T2A-QF2-3XP3-RFP in the *repo* gene crossed to a QUAS-GFP reporter. In 3rd instar larva, the reporter is expressed in the expected glial cells, but also mis-expressed in gut and anal pad (yellow asterisk). (B) T2A-QF2 in the *repo* gene with the 3XP3-RFP removed by Cre-Lox recombination, crossed to a QUAS-GFP reporter. Removal of 3XP3-RFP eliminated gut and anal pad misexpression and did not affect glial cell expression (white arrowheads).

Figure 4: T2A-QF2-T2A-LexA-GAD double driver lines. (A) CRISPR based HDR strategy for integration of the T2A-QF2-T2A-LexA-GAD-3XP3 in the most 5' coding exon common to all or most isoforms, resulting in expression of both activators under control of the endogenous gene regulatory region. The knock-in also produces a truncated endogenous protein and thus a strong loss-of-function allele. If desired, one of the two coding regions can then be excised with Flp, resulting in flies that express only QF2 or LexA-GAD. (B) Alternative strategy allows gene enhancers to be cloned upstream of of T2A-QF2-T2A-LexA-GAD. The vector backbone includes an *attB* site for phiC31 insertion into *attP* flies. (C-D) *T2A-QF2-T2A-LexA-GAD* knock-ins crossed to a QUAS-GFP + LexAop-mCherry double reporter line. (C) The *elav*$^{T2A\text{-}QF2\text{-}T2A\text{-}LexA\text{-}GAD}$ knock-in drives both QUAS-GFP and LexAop-mCherry in the larval brain. There is some leakiness of mCherry in the body wall muscle (arrowheads). (D) The *hh*$^{T2A\text{-}QF2\text{-}T2A\text{-}LexA\text{-}GAD}$ knock-in drives both QUAS-GFP and LexAop-mCherry in the posterior of the wing imaginal disc. GFP expression is much less than mCherry in the wing pouch (asterisks). (E-F) enhancer-T2A-QF2-T2A-LexA-GAD lines crossed to a QUAS-GFP + LexAop-mCherry double reporter line. (E) The *dpp-blk* enhancer-T2A-QF2-T2A-LexA-GAD line drives both QUAS-GFP and LexAop-mCherry along the anterior/posterior boundary of the wing imaginal disc. GFP expression is much less than mCherry in the wing pouch (stars). (F) The *Ilp2* enhancer-T2A-QF2-T2A-LexA-GAD line drives both QUAS-GFP and LexAop-mCherry in the insulin-producing cells of the larval brain (arrows). The fat body mCherry expression (yellow arrowhead) is from leakiness of the reporter stock and does not indicate LexA-GAD activity.

Figure 5: Generation of single drivers from T2A-QF2-T2A-LexA-GAD knock-ins by hs-FLP. (A) FLP/FRT recombination scheme. Flies containing both hs-FLP and a T2A-QF2-T2A-LexA-GAD knock-in are heat shocked during larval development to induce one of two mutually exclusive recombination events in their germline between either FRT or FRT3. (B) heat shock of *hsFLP; hh*$^{T2A\text{-}QF2\text{-}T2A\text{-}LexA\text{-}GAD}$ and hsFLP; *dpp*$^{T2A\text{-}QF2\text{-}T2A\text{-}LexA\text{-}GAD}$ flies produces frequent recombinants, both T2A-QF2 and T2A-LexA-GAD. The bar graph shows the proportion of heat-shocked animals that produced at least one recombinant offspring. The dot plot shows the proportion of recombinant offspring per heat-shocked parent. Mean +/- SD is indicated. (C-D) Validation of individual *hh*$^{T2A\text{-}QF2}$ *and hh*$^{T2A\text{-}LexA\text{-}GAD}$ derivatives by immunofluorescence. All panels show 3rd instar larval wing discs dissected from potential *hh*$^{T2A\text{-}QF2\text{-}T2A\text{-}LexA\text{-}GAD}$ recombinants crossed to a QUAS-GFP + LexAop-mCherry reporter line. (C) Wing disc from non-recombinant *hh*$^{T2A\text{-}QF2\text{-}T2A\text{-}LexA\text{-}GAD}$ showing expression of both GFP and mCherry in the posterior of the wing disc. Note, this is the same image as shown in Figure 4D. (D) Wing disc from recombinant *hh*$^{T2A\text{-}QF2}$ showing expression of GFP but not mCherry in the posterior of the wing disc. (E) Wing disc from recombinant *hh*$^{T2A\text{-}LexA\text{-}GAD}$ showing expression of mCherry but not GFP in the posterior of the wing disc. Validation of (F) *hh*$^{T2A\text{-}QF2}$ *and hh*$^{T2A\text{-}LexA\text{-}GAD}$ derivatives and (G) *dpp*$^{T2A\text{-}QF2}$ *and dpp*$^{T2A\text{-}LexA\text{-}GAD}$ derivatives by PCR from genomic DNA from individual flies. In all panels, for brevity, T2A-QF2-T2A-LexAop, T2A-QF2 and T2A-LexAop, are notated as Q+L, Q(-L) and L(-Q), respectively.

Figure 5—source data 1
Original file for the DNA gel analysis in Figure 5F-G.

Figure 5—source data 2
Original file for the DNA gel analysis with boxes indicating the portions cropped to produce the image for Figure 5F-G.

Figure 6: TRiP LexAop and QUAS shRNA vectors produce effective gene knockdown. (A) shRNAs for knockdown or genes for overexpression were cloned into pLexAop-WALIUM20 and pQUAS-WALIUM20, derived from the TRiP WALIUM20 vector. (B-J) Dorsal view of adult fly thoraces resulting from crosses of LexAop or QUAS shRNAs to *da*$^{T2A\text{-}LexA\text{-}GAD}$ (generated in this study), *Tub-LexA-GAD* (BDSC 66686), or *Tub-QF2* (BDSC 51958). (B-C) *white* shRNA control produced no thoracic phenotypes in any of the crosses. (E-G) *forked* shRNA produced a forked bristles phenotype (white arrowheads). Note that some bristles retain a more elongated wild-type morphology with the Tub-QF2 driven *forked* knockdown (G, yellow asterisk). (H-J) *ebony* shRNA produced a darkened cuticle phenotype. The *da*$^{T2A\text{-}LexA\text{-}GAD}$ driver produced the strongest phenotype (compare panel H to I and J).

Table 1: T2A-LexA-GAD and T2A-QF2 knock-in lines

target tissue	target gene (name)	QF2	this paper	3XP3 removed	others at BDSC	LexA-GAD	this paper	3XP3 removed	others at BDSC
ubiquitous	*da*	yes	yes	yes	no	yes	yes	yes	no
germline	*vas**	yes	yes	no	no	yes	yes	no	no
muscle	*Mef2*	yes	yes	yes	66469	yes	no	yes	97530
muscle	*bt**	yes	yes	no	no	yes	yes	no	no
pan-neuronal	*elav†*	yes	yes	yes	66466	yes	yes	yes	no
glia	*repo*	yes	yes	no	66477	yes	yes	yes	97535
insulin-producing cells	*Ilp2 (regulatory region)†*	yes	yes	N/A	no	yes	yes	N/A	no
fat	*apolpp*	yes	yes	yes	no	yes	yes	yes	no
trachea	*btl*	yes	yes	yes	no	yes	yes	yes	no
heart	*Hand**	yes	yes	yes	no	yes	yes	yes	no
oenocyte	*CG9458**	yes	yes	no	no	yes	yes	yes	no
oenocyte	*CG17560**	yes	yes	no	no	yes	yes	no	no
salivary gland	*Sgs3**	yes	yes	no	no	yes	yes	yes	no
prothoracic gland	*phtm*	yes	yes	yes	no	yes	yes	yes	no
midgut	*mex1*	yes	yes	yes	no	yes	yes	yes	no
adult midgut enterocyte	*Myo31DF*	yes	yes	yes	no	yes	yes	yes	no
hemocyte	*Hml*	yes	yes	yes	66468	yes	yes	yes	no
hemocyte	*He*	yes	yes	yes	no	no	no	N/A	no
crystal cell	*PPO1*	yes	yes	yes	no	yes	yes	yes	no
lamellocyte	*PPO3*	yes	yes	yes	no	yes	yes	yes	no
posterior segment	*hh†*	yes	yes	yes	no	yes	yes	yes	97536
wing pouch/hinge	*nub*	yes	yes	yes	no	yes	yes	yes	no
imaginal disc A/P boundary	*dpp (regulatory region)†*	yes	yes	N/A	no	yes	yes	N/A	no

*constructs were cloned using the Drop-in method. All others were cloned by PCR of long homology arms.

†constructs were cloned into double driver vectors.

Supplementary file 1
Table listing the gene names and antisense sequence of 96 constructs cloned and injected to produce a set of transgenic LexAop-shRNA fly lines.

Supplementary file 2
Table listing the gene names, guide sequences, and primers for amplification of long homology arms for T2A-QF2 and T2A-LexA-GAD constructs.

Supplementary File 3
Sequences of DNA fragments synthesized into the pUC57 Kan_gw_OK2 vector backbone for subsequent Drop-in cloning.

Supplementary File 4
Sequences of DNA fragments used to build pHDR-T2A-QF2-T2A-LexA-GAD and pMCS-T2A-QF2-T2A-LexA-GAD-WALIUM20. FRT3 sequences are shown in blue and FRTwt sequences are shown in red.

Supplementary File 5
Primers and guide sequences for amplification of long homology arms for pHDR-T2A-QF2-T2A-LexA-GAD-3XP3-RFP constructs.

Supplementary File 6
Primers used to amplify large enhancers for cloning into pMCS-T2A-QF2-T2A-LexA-GAD-WALIUM20. The dpp-blk primers have NotI and EcoRI sites for cloning into the MCS, and the Dilp2-enh primers have PacI and EcoRI sites.

Figure 1

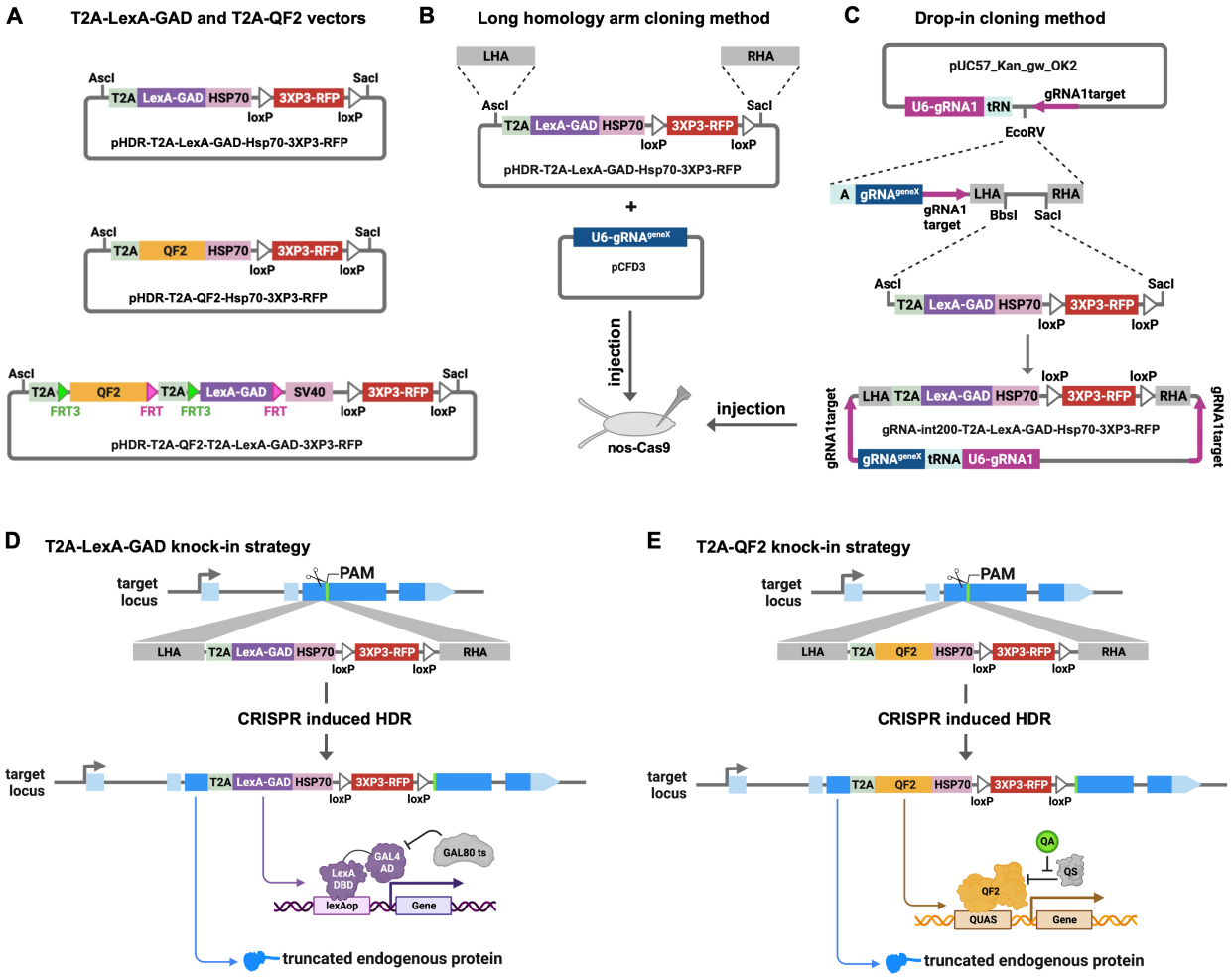
A
T2A-LexA-GAD and T2A-QF2 vectors
AscI
SacI
T2A
LexA-GAD
HSP70
3XP3-RFP
loxP
pHDR-T2A-LexA-GAD-Hsp70-3XP3-RFP
QF2
pHDR-T2A-QF2-Hsp70-3XP3-RFP
FRT3
FRT
SV40
pHDR-T2A-QF2-T2A-LexA-GAD-3XP3-RFP
B
Long homology arm cloning method
LHA
RHA
U6-gRNAgeneX
pCFD3
injection
nos-Cas9
C
Drop-in cloning method
pUC57_Kan_gw_OK2
U6-gRNA1
tRN
gRNA1target
EcoRV
A
gRNAgeneX
gRNA1 target
BbsI
gRNA-int200-T2A-LexA-GAD-Hsp70-3XP3-RFP
D
T2A-LexA-GAD knock-in strategy
target locus
PAM
CRISPR induced HDR
GAL4 AD
GAL80 ts
LexA DBD
lexAop
Gene
truncated endogenous protein
E
T2A-QF2 knock-in strategy
QA
QS
QF2
QUAS

Figure 2

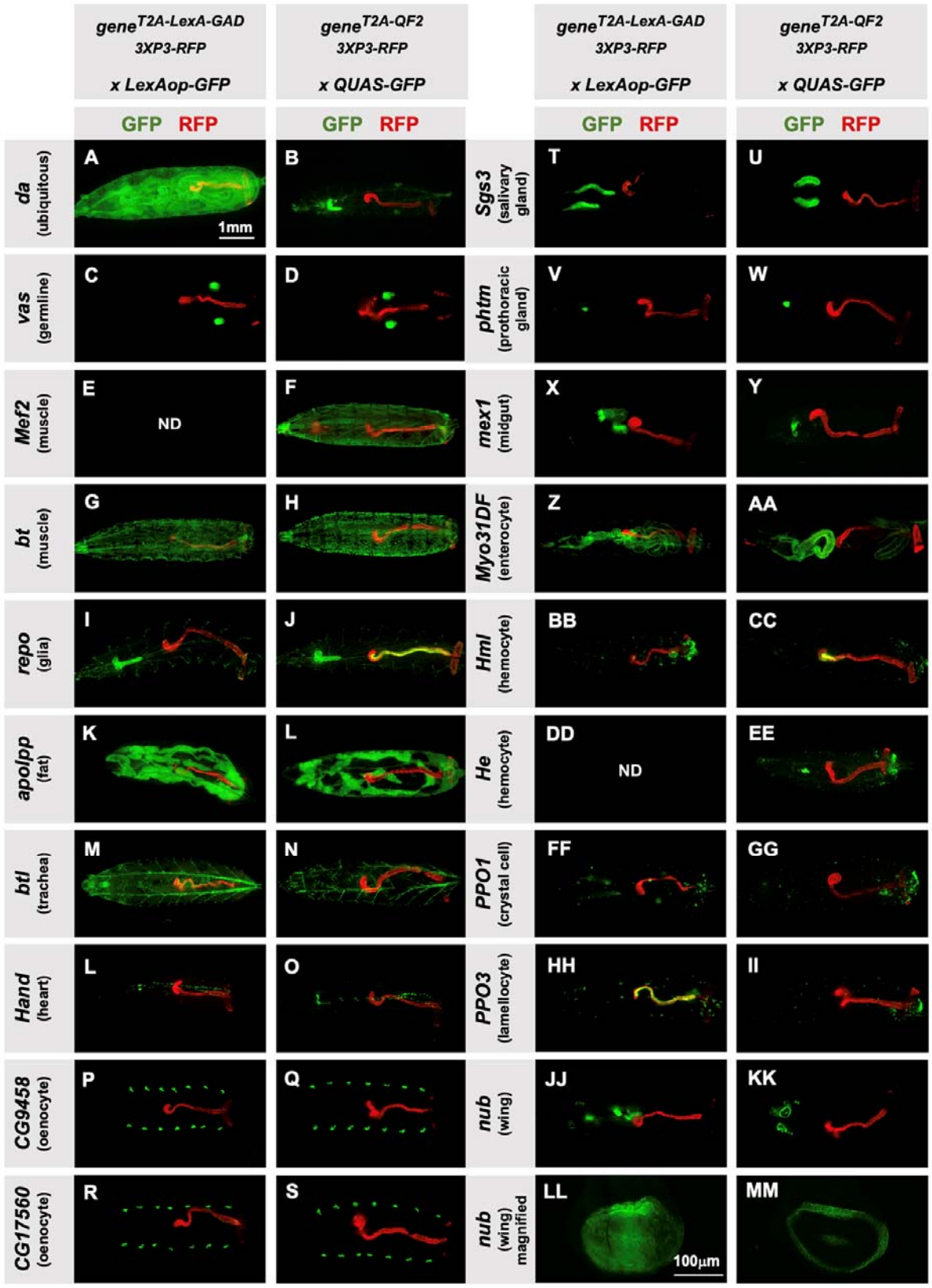
gene T2A-LexA-GAD 3XP3-RFP x LexAop-GFP
gene T2A-QF2 3XP3-RFP x QUAS-GFP
gene T2A-LexA-GAD 3XP3-RFP x LexAop-GFP
gene T2A-QF2 3XP3-RFP x QUAS-GFP
GFP RFP
da (ubiquitous)
vas (germline)
Mef2 (muscle)
bt (muscle)
repo (glia)
apolpp (fat)
btl (trachea)
Hand (heart)
CG9458 (oenocyte)
CG17560 (oenocyte)
Sgs3 (salivary gland)
phtm (prothoracic gland)
mex1 (midgut)
Myo31DF (enterocyte)
Hml (hemocyte)
He (hemocyte)
PPO1 (crystal cell)
PPO3 (lamellocyte)
nub (wing)
nub (wing) magnified
A
B
C
D
E
ND
F
G
H
I
J
K
L
M
N
L
O
P
Q
R
S
T
U
V
W
X
Y
Z
AA
BB
CC
DD
ND
EE
FF
GG
HH
II
JJ
KK
LL
MM
1mm
100µm

Figure 3

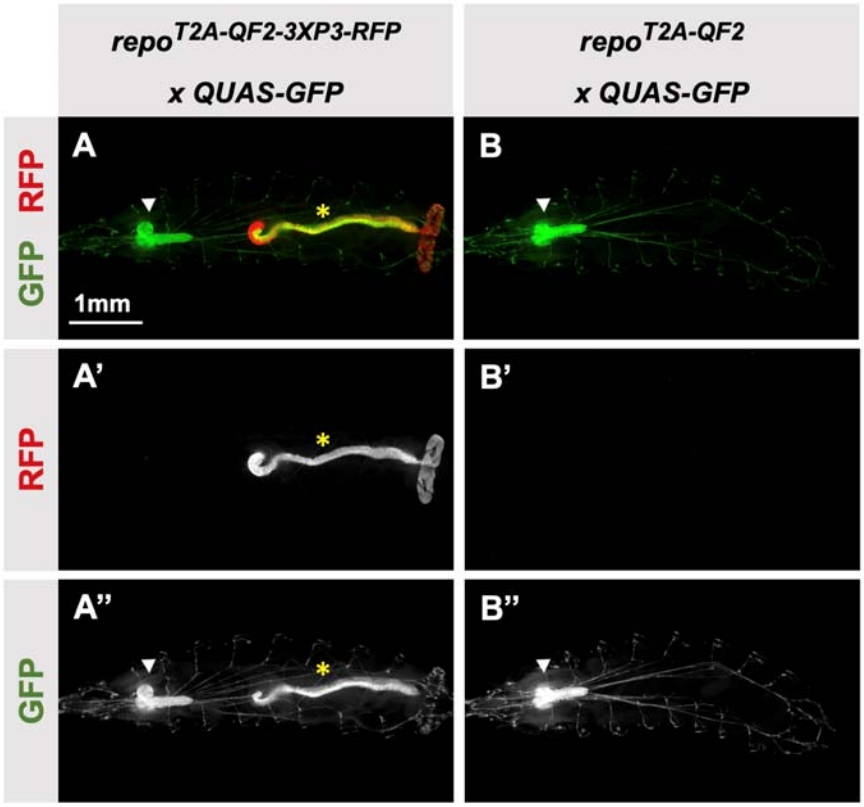
repoT2A-QF2-3XP3-RFP
x QUAS-GFP
repoT2A-QF2
x QUAS-GFP
RFP
GFP
A
B
1mm
RFP
A'
B'
GFP
A"
B"

Figure 4

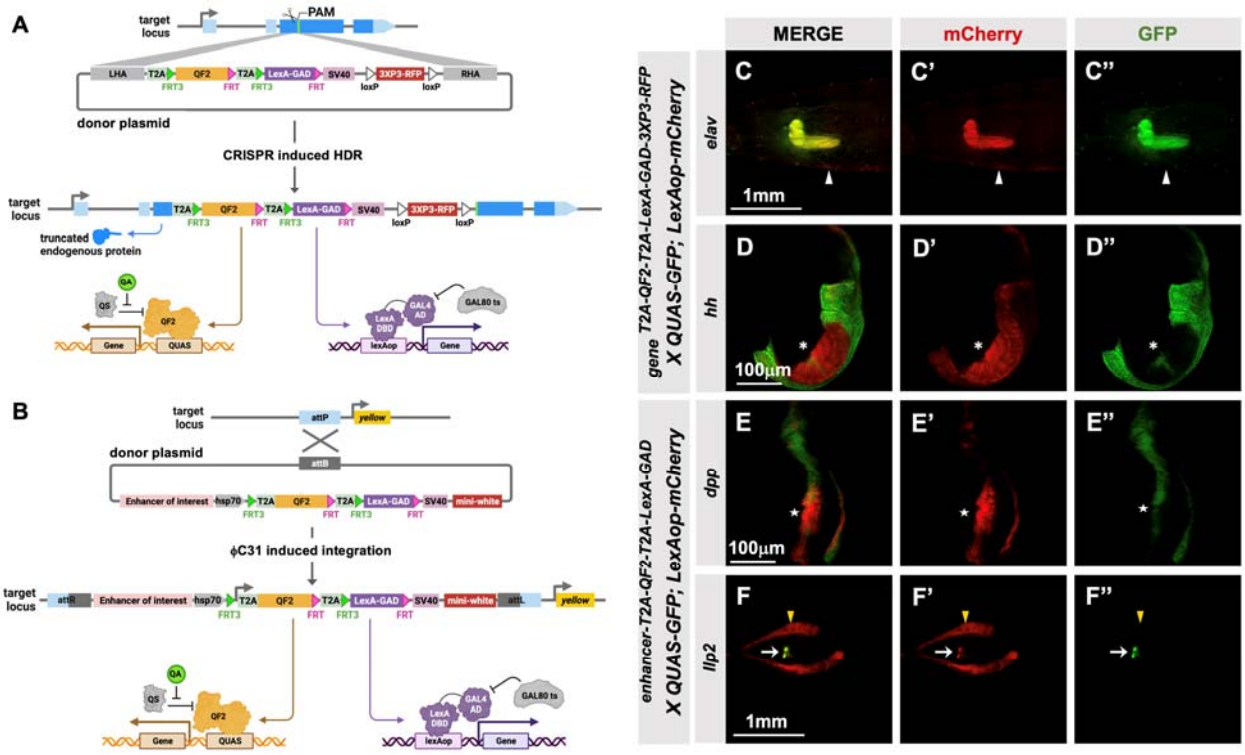
A
target locus
PAM
LHA
T2A
QF2
T2A
LexA-GAD
SV40
3XP3-RFP
RHA
FRT3
FRT
FRT3
FRT
loxP
loxP
donor plasmid
CRISPR induced HDR
target locus
truncated endogenous protein
QA
QS
QF2
Gene
QUAS
GAL4 AD
LexA DBD
GAL80 ts
lexAop
Gene
B
target locus
attP
yellow
donor plasmid
attB
Enhancer of interest
hsp70
T2A
QF2
T2A
LexA-GAD
SV40
mini-white
ϕC31 induced integration
attR
attL
MERGE
mCherry
GFP
gene T2A-QF2-T2A-LexA-GAD-3XP3-RFP X QUAS-GFP; LexAop-mCherry
enhancer-T2A-QF2-T2A-LexA-GAD X QUAS-GFP; LexAop-mCherry
elav
hh
dpp
llp2
C
C'
C''
D
D'
D''
E
E'
E''
F
F'
F''
1mm
100µm
100µm
1mm

Figure 5

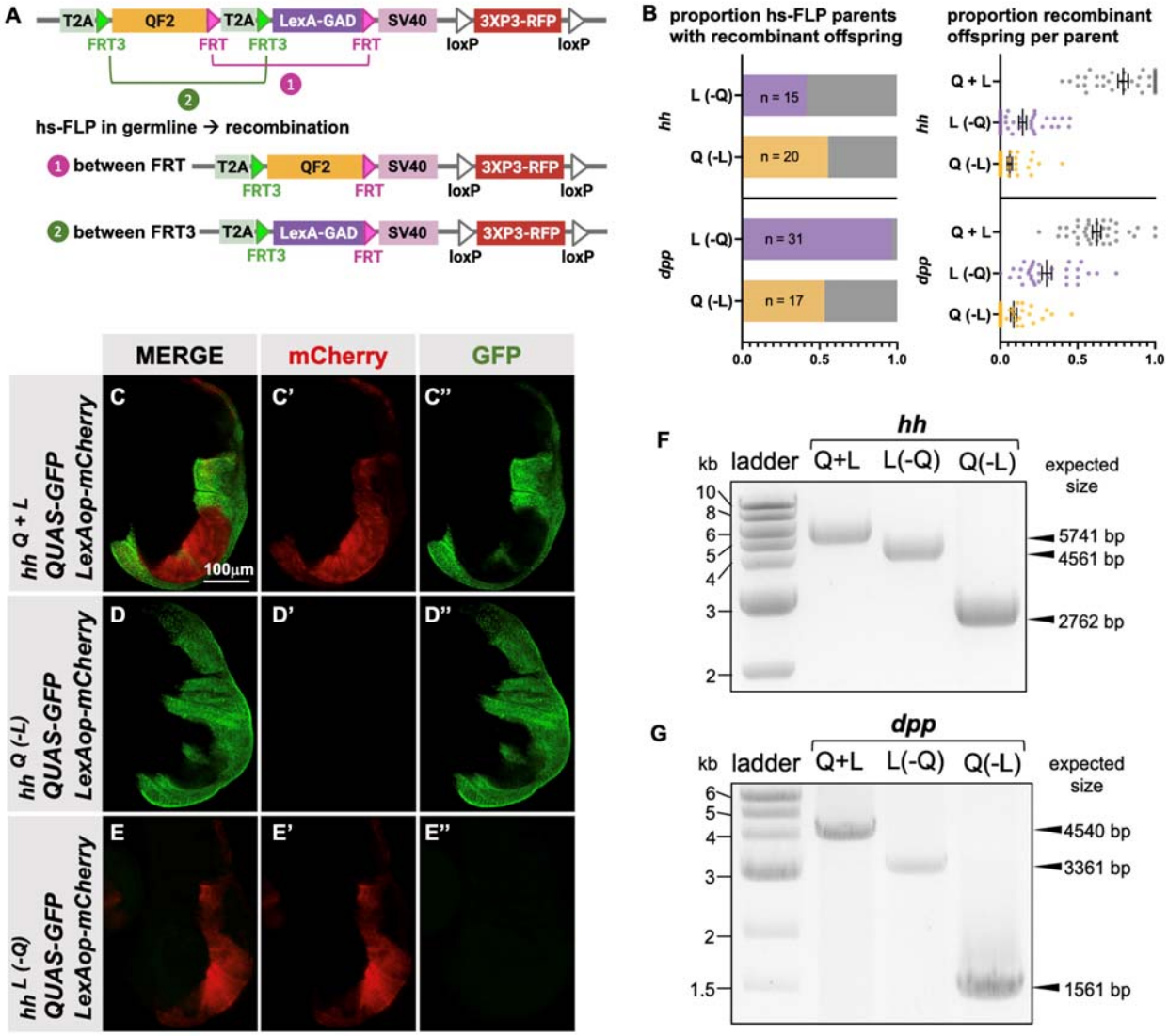
A
T2A
QF2
T2A
LexA-GAD
SV40
3XP3-RFP
FRT3
FRT
FRT3
FRT
loxP
loxP
hs-FLP in germline → recombination
1 between FRT
2 between FRT3
B
proportion hs-FLP parents with recombinant offspring
proportion recombinant offspring per parent
hh
dpp
L (-Q)
Q (-L)
Q + L
n = 15
n = 20
n = 31
n = 17
0.0
0.5
1.0
MERGE
mCherry
GFP
C
C'
C''
D
D'
D''
E
E'
E''
100µm
hh Q + L QUAS-GFP LexAop-mCherry
hh Q (-L) QUAS-GFP LexAop-mCherry
hh L (-Q) QUAS-GFP LexAop-mCherry
F
hh
kb ladder Q+L L(-Q) Q(-L)
expected size
10
8
6
5
4
3
2
5741 bp
4561 bp
2762 bp
G
dpp
kb ladder Q+L L(-Q) Q(-L)
expected size
6
5
4
3
2
1.5
4540 bp
3361 bp
1561 bp

Figure 6

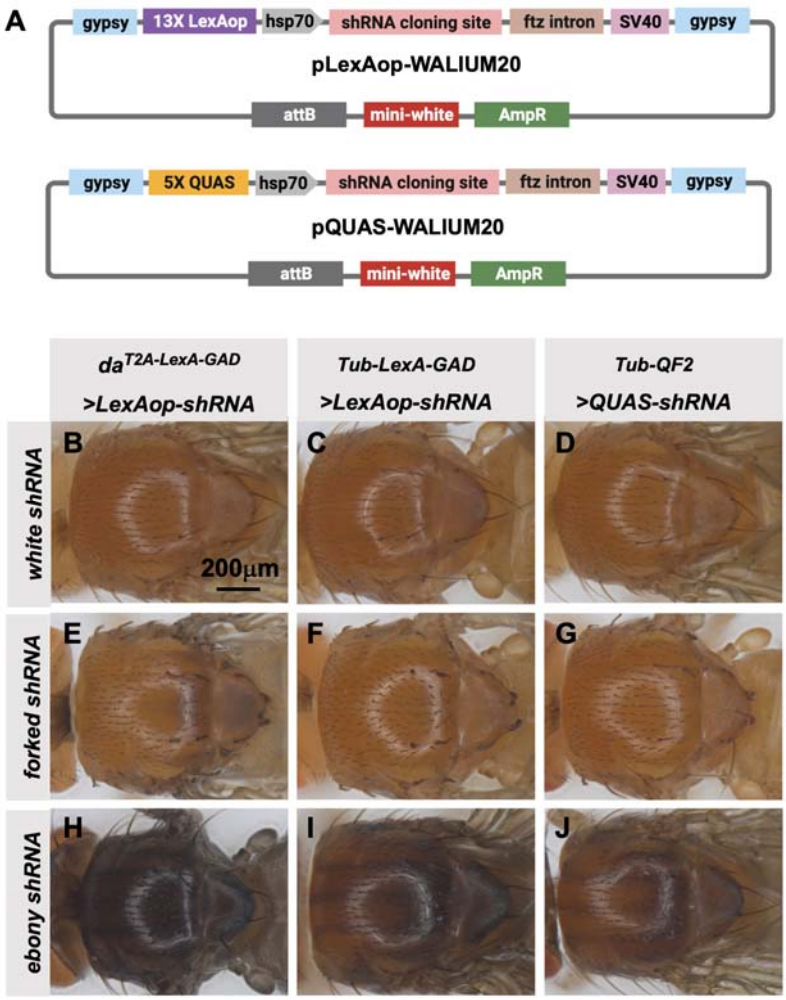
A
gypsy
13X LexAop
hsp70
shRNA cloning site
ftz intron
SV40
gypsy
pLexAop-WALIUM20
attB
mini-white
AmpR
gypsy
5X QUAS
hsp70
shRNA cloning site
ftz intron
SV40
gypsy
pQUAS-WALIUM20
attB
mini-white
AmpR
daT2A-LexA-GAD
>LexAop-shRNA
Tub-LexA-GAD
>LexAop-shRNA
Tub-QF2
>QUAS-shRNA
white shRNA
forked shRNA
ebony shRNA
B
C
D
E
F
G
H
I
J
200μm